Dear Author,

Please, note that changes made to the HTML content will be added to the article before publication, but are not reflected in this PDF.

Note also that this file should not be used for submitting corrections.

Biochimica et Biophysica Acta xxx (2016) xxx–xxx

Contents lists available at ScienceDirect

Biochimica et Biophysica Acta

journal homepage: www.elsevier.com/locate/bbamem

Interaction of lipids with the neurotensin receptor 1

Juan H. Bolivar, Juan C. Muñoz-García, Tomas Castro-Dopico, Patricia M. Dijkman, Phillip J. Stansfeld, Anthony Watts *

Biomembrane Structure Unit, Department of Biochemistry, University of Oxford, South Parks Road, Oxford OX1 3QU, UK

ARTICLE INFO

Article history:
Received 1 October 2015
Received in revised form 2 February 2016
Accepted 24 February 2016
Available online xxxx

Keywords:
Neurotensin
GPCR
Lipids
Oligomerization
ESR

ABSTRACT

Information about lipid–protein interactions for G protein-coupled receptors (GPCRs) is scarce. Here, we use electron spin resonance (ESR) and spin-labelled lipids to study lipid interactions with the rat neurotensin receptor 1 (NTS1). A fusion protein containing rat NTS1 fully able to bind its ligand neurotensin was reconstituted into phosphatidylcholine (PC) bilayers at specific lipid:protein molar ratios. The fraction of motionally restricted lipids in the range of 40:1 to 80:1 lipids per receptor suggested an oligomeric state of the protein, and the result was unaffected by increasing the hydrophobic thickness of the lipid bilayer from C-18 to C-20 or C-22 chain length PC membranes. Comparison of the ESR spectra of different spin-labelled lipids allowed direct measurement of lipid binding constants relative to PC (K_r), with spin-labelled phosphatidylethanolamine (PESL), phosphatidylserine (PSSL), stearic acid (SASL), and a spin labelled cholesterol analogue (CSL) K_r values of 1.05 ± 0.05, 1.92 ± 0.08, 5.20 ± 0.51 and 0.91 ± 0.19, respectively. The results contrast with those from rhodopsin, the only other GPCR studied this way, which has no selectivity for the lipids analysed here. Molecular dynamics simulations of NTS1 in bilayers are in agreement with the ESR data, and point to sites in the receptor where PS could interact with higher affinity. Lipid selectivity could be necessary for regulation of ligand binding, oligomerisation and/or G protein activation processes. Our results provide insight into the potential modulatory mechanisms that lipids can exert on GPCRs.

1. Introduction

Several studies have shown that GPCR function is affected by the lipid environment (reviewed in ref. [1–4]), with most reports focusing on the role of cholesterol and lipid microdomains influencing receptor activity, localisation, and G protein coupling in celulla. However, the molecular mechanisms that govern these interactions are poorly understood, and there is little information on how specific lipid species interact with GPCRs in membranes. This is due to the technical challenges associated with expression [5,6], purification [7–9] and reconstitution [10–16] of GPCRs into model bilayers that allow controlled, specific analysis of lipid–protein interactions, and then comparison with functional assays. This type of detailed information is essentially limited to rhodopsin [17–20], which functions in the very specific membrane environment of the outer rod segment. The purpose here is to extend this knowledge for another prototype GPCR of pharmacological relevance, the neurotensin receptor 1 (NTS1).

Neurotensin is a tridecapeptide that functions as a neurotransmitter or neuromodulator in the central nervous system and as a local hormone in peripheral tissues. Three different receptors have been identified for neurotensin, namely NTS1, NTS2 and NTS3, of which NTS1 is the principal mediator of the known effects of neurotensin. The neurotensin receptor 1 belongs to the group A of GPCRs and homologues have been described in mammals (mouse, rat, humans), amphibians, fish and birds [21,22]. In rat, NTS1 is found in distinctive areas of the brain [23–26] and spinal cord [27] as well as in the heart, duodenum, small intestine, large intestine, and liver [23]. A wide distribution is also seen in humans [28] and other species [21]. Through its roles in central nervous system NTS1 has been associated with several neurological disorders [29]. It has also been found to play a role in cell proliferation and cancer, and is a potential biomarker [30] and target [31] in cancer therapy.

Abbreviations: CHS, cholesterol hemisuccinate; CHAPS, 3-[(3-cholamidopropyl)-dimethylammonio]-1-propanesulfonate; CSL, 4′,4′-dimethylspiro(5α-cholestane-3,2′-oxazolidin)-3′-yloxyl; C14:0PC, 1,2-dimyristoyl-*sn*-glycero-3-phosphocholine; C15:0PC, 1,2-dipentadecanoyl-*sn*-glycero-3-phosphocholine; C16:0–C18:1PC, 1-palmitoyl-2-oleoyl-*sn*-glycero-3-phosphocholine; C16:0–C18:1PE, (1-palmitoyl-2-oleoyl-*sn*-glycero-3-phosphoethanolamine); C16:0–C18:1PS, (1-palmitoyl-2-oleoyl-*sn*-glycero-3-phospho-L-serine); C18:1PC, 1,2-dioleoyl-*sn*-glycero-3-phosphocholine; C20:1PC, 1,2-dieicosenoyl-*sn*-glycero-3-phosphocholine; C22:1PC, 1,2-dierucoyl-*sn*-glycero-3-phosphocholine; DDM, n-dodecyl-β-D-maltoside; ESR, electron spin resonance; GPCR, G protein-coupled receptor; MBP, maltose binding protein; NTS1, neurotensin receptor 1; PC, phosphatidylcholine; PE, phosphatidylethanolamine; PS, phosphatidylserine; rPE, 1,2-dioleoyl-*sn*-glycero-3-phosphoethanolamine-N-(lissamine rhodamine B sulfonyl); SA, stearic acid; TM, transmembrane helix; 14-PCSL, 1-acyl-2-[14-(4,4-dimethyloxazolidinyl-*N*-oxyl) stearoyl]-*sn*-glycero-3-phosphocholine; 14-PESL, 1-acyl-2-[14-(4,4-dimethyloxazolidinyl-*N*-oxyl)stearoyl]-*sn*-glycero-3-phosphoethanolamine; 14-PSSL, 1-acyl-2-[14-(4,4-dimethyloxazolidinyl-*N*-oxyl)stearoyl]-*sn*-glycero-3-phosphoserine; 14-SASL, 14-(4,4-dimethyloxazolidinyl-*N*-oxyl)stearic acid.

* Corresponding author.
E-mail address: anthony.watts@bioch.ox.ac.uk (A. Watts).

http://dx.doi.org/10.1016/j.bbamem.2016.02.032
0005-2736/

The wide tissue distribution of NTS1 and its involvement in numerous physiological and pathological processes highlight the extreme complexity of this receptor and anticipate an exquisite regulation of its functions at the molecular level. NTS1 is able to activate a range of signalling pathways through interaction with $G_{q/11}$ at its intracellular loop 3 (IC3) [32], and through interaction with $G_{i/o}$ and G_s at the first half of its C-terminal portion [33,34] and a recent study shows that this is complicated by the possible $G_{\alpha\beta\gamma}$ heterotrimers that can interact with NTS1 [35]. Some transduction pathways can be suppressed by mutation or deletion of particular intracellular domains while leaving unrelated pathways intact, suggesting that pathways can be individually regulated by direct interactions with the receptor [36]. Further complexity is added when considering the potential functional consequences from receptor homo- [10,11] or heterodimerisation [37,38], and modifications such as phosphorylation, acylation and glycosylation [39]. Finally, when considering the various lipid environments that NTS1 can experience in different cell types, the possibility arises that receptor function could be fine-tuned to serve particular cell type requirements according to cell type membrane composition, adding an extra dimension of complexity to receptor modulation.

Recently, we showed that binding of neurotensin to NTS1, receptor homodimerisation, and coupling to $G_{\alpha i1}$ are greatly affected by the specific lipid composition of the bilayer [40,41], and Grisshammer and co-workers showed that the same holds for G_q protein activation [12]. Here, we now analyse how major lipid species of the mammalian plasma membrane interact with the transmembranous region of rat NTS1 using a fusion protein termed NTS1-B. We present a protocol for reconstituting NTS1-B at low lipid to protein molar ratios in a controlled manner which allows us to measure directly interactions of spin-labelled lipids with the receptor using electron spin resonance (ESR).

2. Materials and methods

2.1. Materials

The phospholipids, 1,2-dioleoyl-*sn*-glycero-3-phosphocholine (C18:1PC), 1,2-dieicosenoyl-*sn*-glycero-3-phosphocholine (C20:1PC), 1,2-dierucoyl-*sn*-glycero-3-phosphocholine (C22:1PC) and 1,2-dioleoyl-*sn*-glycero-3-phosphoethanolamine-N-(lissamine rhodamine B sulfonyl) (rPE) were obtained from Avanti Polar Lipids. The spin-labelled phospholipids 1-acyl-2-[14-(4,4-dimethyloxazolidinyl-*N*-oxyl)stearoyl]-*sn*-glycero-3-phosphocholine (14-PCSL), 1-acyl-2-[14-(4,4-dimethyloxazolidinyl-*N*-oxyl)stearoyl]-*sn*-glycero-3-phosphoethanolamine (14-PESL), and 1-acyl-2-[14-(4,4-dimethyloxazolidinyl-*N*-oxyl)stearoyl]-*sn*-glycero-3-phosphoserine (14-PSSL), and the spin-labelled fatty acid 14-(4,4-dimethyloxazolidinyl-*N*-oxyl)stearic acid (14-SASL) were synthesized as described by Marsh and Watts [42]. The spin-labelled cholesterol analogue 4′,4′-dimethylspiro(5α-cholestane-3,2′-oxazolidin)-3′-yloxyl (CSL), cholesterol hemisuccinate (CHS) and sodium cholate were obtained from Sigma-Aldrich. The detergents, 3-[(3-cholamidopropyl)-dimethylammonio]-1-propanesulfonate (CHAPS), and n-dodecyl-β-D-maltoside (DDM) were from Melford Laboratories.

2.2. Protein production

The plasmid with the rat NTS1-B construct (MBP-N10-Tev-rT43NTR-CH2-N5G3S-G3S-TrxA-H10) was a gift of Dr. Grisshammer and is described in ref. [7]. The construct consists of the *E. coli* maltose binding protein (MBP, residues Lys^1 to Thr^{366}), a GSN_{10}ENLYFQSGS linker including a tobacco etch virus (Tev) cleaving recognition site (underlined), the rat NTS1 (residues Thr^{43} to Tyr^{424}), a $FQSN_5G_3SG_3SEF$ linker containing part of a second Tev cleaving recognition site which starts in the C-terminus of NTS1, followed by the *E. coli* thioredoxin (Trx, residues Ser^2 to Ala^{109}), and a GT link to a ten histidine tag. Expression and purification protocols have been extensively described [5,8]. NTS1-B was expressed in *E. coli* BL21 (DE3) cells. All steps were performed at 4 °C or on ice and when required between days along the protocol the sample was frozen in liquid N_2 and stored −80 °C. Cell pellets were solubilised with buffer A [50 mM Tris pH 8 (4 °C), 30% glycerol (*v*/v)] containing 200 mM NaCl, 0.1% CHS, 0.5% CHAPS, and 1% DDM (*w*/*v* in all cases for the detergents) and in the presence of protease inhibitors, lysozyme and DNAase. Insolubilised material was discarded after centrifugation (60 min; 65,000 *g*) and NTS1-B was purified first through a 5 ml Ni-NTA column eluting in buffer A with 350 mM imidazole, 200 mM NaCl, 0.1% CHS, 0.5% CHAPS, and 0.1% DDM. The eluate was diluted with buffer A containing 0.1% DDM and 0.01% CHS to reach 50 mM NaCl and then further purified through a neurotensin ligand affinity column. Pure NTS1-B was eluted in buffer A with 1 M NaCl, 0.1% DDM and 0.01% CHS. Fractions were frozen in liquid N_2 and stored at −80 °C.

2.3. Reconstitution into bilayers

The required amount of lipid from chloroform stocks was dried in glass vials as a thin film under a stream of N_2, then under vacuum ($<10^{-5}$ Torr) overnight. The lipid film was resuspended in buffer B [50 mM Tris pH 8 (4 °C), 50 mM NaCl] with 1 mM EDTA and the necessary concentration of sodium cholate to achieve 20 mM final concentration after addition of the receptor to the solubilised lipid. The resuspended lipid was fully solubilised to clarity in a bath sonicator (9 min; Langford Sonomatic Ultrasonics 475H). Purified NTS1-B was first concentrated by binding it to a 1 ml Ni-NTA column at a slow flow rate (rebinding the flow through once more markedly increased the amount of protein bound). The bound protein was washed with 50 ml of buffer B containing 0.1% DDM (*w*/*v*) to eliminate CHS. The receptor was eluted with 350 mM imidazole and the concentration determined by absorbance at 280 nm using a molar extinction coefficient of 138,785 cm^{-1} M^{-1} as calculated [43], using the ExPasy ProtParam Tool [44]. Subsequently, the appropriate amounts of solubilised lipid and protein were mixed to achieve the desired lipid:protein molar ratio. At this point, 2 mol% spin-labelled lipid (with respect to total lipid) was added to the mixture from ethanol stocks (except in the case of 14-SASL, which must be added later as it is otherwise lost in posterior dilution/dialysis), the final ethanol concentration in the mixture being lower than 1% (*v*/v), as described previously [17]. In the case of the samples for determination of relative lipid binding constants, a large sample was first prepared by mixing lipid and protein, and only then was the sample split into identical aliquots to which the required spin-labelled lipids were added (only 14-SASL was added later). This was to ensure the lipid:protein molar ratio in each of these samples was identical. Reconstitution was performed by 100 fold dilution with buffer B with 1 mM EDTA taking the detergents below their critical micelle concentration. Any remaining detergent was eliminated by extensive dialysis against 100× the sample volume (24 h; 4 °C) replacing the buffer after approximately 3 h and 7 h. Note that generally only 0.5–1 mol% spin-labelled lipid is necessary, but during dialysis about 50% becomes reduced so that it is necessary initially to add an excess. Reconstituted proteoliposomes were collected by ultracentrifugation (100,000 *g*; 2 h; 4 °C) and resuspended in about 1.5 ml of buffer B with 1 mM EDTA. A small sample was taken for determination of the final lipid:protein molar ratio, and 0.5 mol% 14-SASL was added to the corresponding sample from an ethanol stock ensuring that the final ethanol concentration was below 1%. Proteoliposomes were pelleted in a bench top centrifuge, loaded into 50 μl glass capillaries for ESR measurements, snap frozen in liquid N_2 and kept at −80 °C until the day of measurement.

2.4. Determination of lipid:protein molar ratio by absorbance spectroscopy

For determination of the final lipid:protein molar ratio in each sample, rPE was initially mixed with the lipids in chloroform prior to

Please cite this article as: J.H. Bolivar, et al., Interaction of lipids with the neurotensin receptor 1, Biochim. Biophys. Acta (2016), http://dx.doi.org/10.1016/j.bbamem.2016.02.032

drying the lipid films so that after later incorporation of protein a rPE:NTS1-B molar ratio of 0.85:1 would be obtained, resulting in 2.1 mol% or less rPE in the total lipid, depending on the total lipid:protein molar ratio. Thus, after reconstitution an absorption spectrum could be measured simultaneously for rPE (573 nm) and protein (280 nm). Assuming that the rPE to host lipid ratio remains constant during sample preparation, the final lipid:protein molar ratio can be readily calculated. Such assumption is safe because the resulting proteoliposomes are homogeneous in lipid:protein ratio, which shows homogeneous mixing of lipid and protein (see results Fig. S2), and because the preparative lipid:protein ratios at the start and the final lipid:protein ratios determined by absorbance are closely matched for all the samples (see results Table 1). The molar extinction coefficient of lissamine rhodamine B sulphonyl chloride of 88,000 cm^{-1} M^{-1} (Molecular Probes Handbook, Invitrogen) was taken for rPE, with the absorption maximum occurring at 573 nm in 1% SDS for rPE. After protein reconstitution, a small aliquot of sample was diluted 2.5× into a final concentration of 1% SDS to reduce scattering from the lipid vesicles. A blank of lipid prepared the same way in the absence of protein was used to subtract residual scattering and rPE absorbance at 280 nm [16].

2.5. ESR spectroscopy

Continuous wave ESR measurements were performed on an X-band Bruker EMX spectrometer. Spectra were recorded at 18 and 25 °C, which are well above the lipid phase transition temperature of the PC bilayers used. The slow and fast motion components in the composite spectra were determined by spectral addition as described in refs. [45,46]. Single-component spectra libraries were obtained from 14-PCSL in C18:1PC membranes recorded from 2 to 35 °C at 1 °C intervals for the fast motion component, and from 14-PCSL in sonicated C14:0PC (1,2-dimyristoyl-*sn*-glycero-3-phosphocholine) membranes recorded from 0 to 20 °C at 3 or 4 °C intervals for the slow motion component. For analysis of the CSL sample in particular, single-component spectra from libraries of CSL in C18:1PC (fast motion) and in sonicated C14:0PC (slow motion) membranes were used.

2.6. Sucrose density analysis

After ESR measurements, samples were resuspended in 200 μl buffer B and were subject to a discontinuous sucrose density gradient from 20 to 65% (*w*/*v*) sucrose in buffer B with increasing 1 ml steps of 5%. Gradients were centrifuged (100,000 *g*; 4 °C, 18 h) in a swing rotor (Beckman SW41 Ti).

Table 1
Lipid:NTS1-B molar ratios, fraction of slow motion component in the ESR spectra from 14-PCSL, and derived N_b values for each reconstituted sample. The final lipid:NTS1-B molar ratios after reconstitution were determined measuring simultaneously absorbance at 573 nm and 280 nm for rPE and NTS1-B, respectively. ESR measurements were recorded at 25 °C or 18 °C (†) to facilitate spectral analysis. The error is the maximum range of error introduced upon determination of the final lipid:protein molar ratio (N_t) and the fraction of immobile component (f). The error for the N_b values is the maximum difference between the N_b value and the value obtained when N_b is calculated taking the extreme error values for N_t and f. (*) Combined sample used for measuring relative lipid affinities for which the corresponding sucrose density gradient analysis is also marked (*) in Fig. S2; the fraction of slow motion component is only given here for 14-PCSL.

Lipid	Preparative lipid:NTS1-B molar ratio	Final lipid:NTS1-B molar ratio	Fraction of slow motion component (f)	Average number of lipid molecules associated to a NTS1-B molecule (N_b)
C18:1PC	80:1	75 ± 6:1	0.14 ± 0.05†	11 ± 5
C18:1PC	60:1	57 ± 5:1	0.23 ± 0.01†	13 ± 2
C18:1PC	50:1	43 ± 3:1	0.23 ± 0.03†	10 ± 2
C18:1PC	40:1	39 ± 5:1	0.30 ± 0.01†	12 ± 2
C18:1PC*	40:1	33 ± 3:1	0.29 ± 0.01	10 ± 1
C20:1PC	40:1	41 ± 5:1	0.34 ± 0.02	14 ± 3
C22:1PC	40:1	36 ± 6:1	0.28 ± 0.03	10 ± 3

2.7. Molecular dynamics (MD) simulations

Simulations were run using GROMACS (v. 4.6.3) [47]. A self-assembly coarse grained (CG) MD simulation [48] in a C16:0–C18:1PC (1-palmitoyl-2-oleoyl-*sn*-glycero-3-phosphocholine) membrane was first performed for 100 ns at 323 K, giving a protein-embedded membrane of about 300 C16:0–C18:1PC lipid molecules, solvated with SPC water molecules [49], and containing around 150 mM NaCl. The NTS1 crystal structure of PDB ID: 4BUO [50] was employed upon ligand removal. R305 was back-mutated to H305 and the non-resolved intracellular loop 1 (IC1) was modelled using the software Modeller [51]. To build the brain polar lipid (BPL) bilayer model, the self-assembled C16:0–C18:1PC CG system was lipid-exchanged [52] to C16:0–C18:1PC, C16:0–C18:1PS (1-palmitoyl-2-oleoyl-*sn*-glycero-3-phospho-L-serine), C16:0–C18:1PE (1-palmitoyl-2-oleoyl-*sn*-glycero-3-phosphoethanolamine) and cholesterol at a PC:PS:PE:cholesterol molar ratio of 15:22:39:24 to approximately mimic the BPL lipid composition (Avanti catalogue No. 141101; and assuming a 24% in cholesterol content). The resulting heterogeneous membrane system was submitted to a 1-microsecond CG-MD simulation at 323 K using the same parameters as for the C16:0–C18:1PC CG-MD. The final system was then converted to atomistic (AT) detail using the CG2AT protocol [53], then bilayer/solvent equilibrated (positional restraints on the protein) for 1 ns [54], and finally run for a further 200 ns (at 323 K) of AT-MD with the GROMOS96 53a6 force field.

The atomistic system was considered to be in equilibrium after the first 20 ns of AT-MD, based on NTS1 backbone RMSD (Fig. S1). The trajectory analysis was performed from 20 ns to 200 ns using GROMACS and VMD tools.

3. Results

3.1. Reconstitution of NTS1-B in lipid bilayers

Analysis of lipid–protein interactions using ESR and spin-labelled lipids requires proteoliposomes that are homogeneous in lipid:protein content and a knowledge of the lipid:protein molar ratio. This is necessary to ensure a homogeneous equilibrium of lipid–protein interactions across the sample, to enable measurement of the relative lipid binding constants. Fig. S2 shows sucrose density gradients of NTS1-B reconstituted into lipid bilayers by a dilution-dialysis method. Samples were doped with rPE to allow easy visualisation of the proteoliposomes and to quantify the lipid content by absorbance spectroscopy. The sharp bands show that all samples were homogeneous in density and therefore homogeneous in lipid:protein content. Increasing the lipid:protein molar ratio decreased the density of the proteoliposomes, which ran higher in the gradient. It can be seen that the proteoliposomes do not run exactly at the interface between the gradient steps, particularly the sample of lipid:protein molar ratio of 50:1 which runs in the middle of the 40% sucrose step. This indicates that the gradient becomes continuous during centrifugation, although the steepness of the gradient formed between the steps might vary. Reconstitution of NTS1 cleaved from its fusion partners (MBP, Trx) gave heterogeneous proteoliposomes (Fig. S2). The reduced hydrophilicity of the cleaved protein might influence the reconstitution process, and thus ESR experiments were performed with the full NTS1-B construct. NTS1-B has MBP and Trx fused at its N- and C-terminus, respectively. The topology of the receptor, with its N-terminus coming out of one side of the membrane and its C-terminus coming out of the other side, means that its water soluble fusion partners are located at opposite sides of the bilayer. Strong evidence that the fusion partners are not embedded in the bilayer (as expected) comes from the fact that it is possible to cleave them free also when the protein is reconstituted in lipid bilayers (nanodiscs) [12]. Therefore, MBP and Trx are not expected to alter interactions of lipids with the transmembranous region of NTS1. The NTS1-B fusion protein maintains a biologically relevant fold as evident from its

Please cite this article as: J.H. Bolivar, et al., Interaction of lipids with the neurotensin receptor 1, Biochim. Biophys. Acta (2016), http://dx.doi.org/10.1016/j.bbamem.2016.02.032

ability to bind to neurotensin in the neurotensin affinity column, and previous experiments with the receptor also fused to MBP at the N-terminal side and fused to different G proteins at the C-terminal side showed that the fusion protein retained its ability to activate G proteins [55]. Therefore studies of lipid–protein interactions in NTS1-B are representative of lipid interactions with the native receptor. Table 1 shows the spectrophotometric analysis of the proteoliposomes, and the final lipid:protein molar ratios, which were very close to the intended preparative values as expected, given the homogeneity of the samples. These values were used to calculate the average number of lipids associated with the transmembrane region of a NTS1-B molecule, as described below.

3.2. The lipid–protein interface

Interaction of spin-labelled lipids with the transmembranous region of a protein reduces the motion of the spin label compared to that in the bulk bilayer, so that the anisotropic averaging of the spin label is reduced for the population of lipids in contact with the protein interface, giving a broader ESR spectrum that can be resolved from the narrower spectrum of the lipids in the bulk bilayer, as shown for many other examples [17,42,45]. The host lipid C18:1PC was chosen for these studies for its low phase transition temperature (−17 °C) to ensure maximum miscibility with other lipid species and with the protein, and because PC is one of the main components of mammalian plasma membranes [56]. Fig. 1 shows the ESR spectrum of 14-PCSL in C18:1PC membranes containing NTS1-B at a lipid:protein molar ratio of 40:1. The spectrum shows two components: a narrow component (dashed arrows) from 14-PCSL in the bulk bilayer, and a broad component (solid arrows) from 14-PCSL in contact with the transmembranous region of NTS1-B. For comparison, the spectra of 14-PCSL in 18:1PC membranes (Fig. 1C) and in sonicated C14:0PC membranes (Fig. 1B) in the absence of protein are shown. In the absence of protein, in C18:1PC membranes the spectrum is narrow indicating fast anisotropic averaging of the spin label, while in saturated C14:0PC membranes the spectrum is wider due to less complete anisotropic averaging. The motional averaging of these single-component spectra matches that in the two-component spectrum, so that the single-component spectra fitted together to match the two-component spectrum (Fig. 1A, dashed line) give the fractions of slow (0.30 ± 0.01) and fast (0.70 ± 0.01) motion spin-labelled lipids in the two-component spectrum [42,45], showing that 30 ± 1% of 14-PCSL is in contact with the receptor.

From the lipid:protein molar ratio (N_t) of a sample, and the fraction of slower motion component (f) in the ESR spectrum of the spin-labelled lipid, it is possible to determine the average number of lipid molecules that are interacting with a single protein molecule (N_b), as shown for several other proteins [42,45,57,58]. At the low concentrations of spin-labelled lipids ($<<N_t$) this relation is described by:

$$[(1-f)/f] = (1/K_r)[(N_t/N_b)-1] \quad (1)$$

where K_r is the relative affinity for the protein of the spin-labelled lipid relative to the unlabelled lipid. At $[(1-f)/f] = 0$, $N_t = N_b$, giving the number of motionally restricted lipids interacting with the protein [42,45]. In Fig. 2, the experimental data obtained for 14-PCSL in membranes of increasing lipid:NTS1-B molar ratios is fitted to Eq. 1. It is not expected that 14-PCSL shows any specific interaction for a protein when in a PC bilayer, as shown previously [42,45] so that it is sensible to assume $K_r^{PC} = 1$ (where K_r^{PC} is K_r for 14-PCSL relative to C18:1PC). The N_b value given at the intercept of $[(1-f/f)] = 0$ is 11 ± 1 (Fig. 2). By

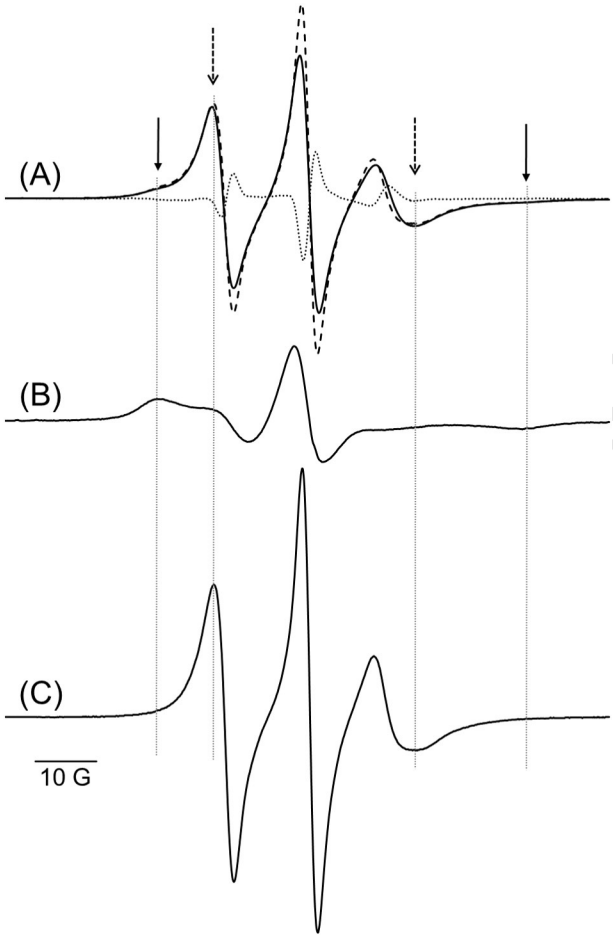

Fig. 1. Single column fitting. ESR spectra of 14-PCSL: (A) in C18:1PC membranes containing NTS1-B at a lipid:protein molar ratio of 40:1 (solid line); (B) in C14:0PC sonicated membranes; (C) in C18:1PC membranes. In (A), the single-component spectra shown in (B) and (C) were fitted to the two-component spectrum (solid line) obtained in the presence of NTS1-B. The resulting fitted spectrum is in dashed line, and the dotted line is the subtraction of the fitted spectrum from the experimental spectrum. Small differences between the experimental and fitted spectra are normally seen in the regions of steep slope due to small differences in motional averaging. Solid arrows point to the outer peaks from the slow motion component, and dashed arrows point to the outer peaks from the fast motion component. For comparison, vertical dotted lines trace the positions of the peaks along all the spectra. Measurements were recorded at 25 °C (A), 4 °C (B) and 18 °C (C), with a total scan width of 150 G. The spectra are normalized to equal second integrals.

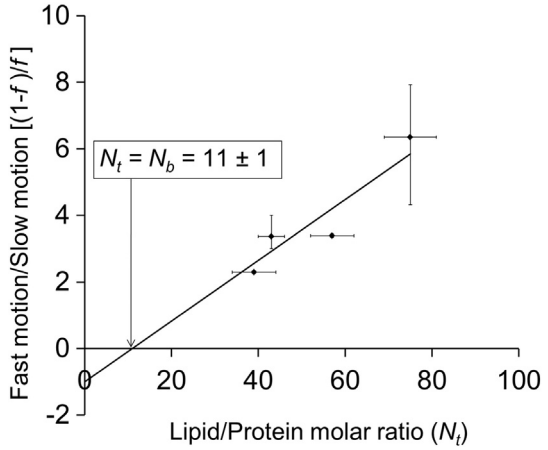

Fig. 2. Single column fitting. Ratio of fast to slow motion populations of 14-PCSL as a function of lipid:protein molar ratio. The fractions of slow (f) and fast ($1-f$) motion 14-PCSL were obtained from the 14-PCSL spectra in samples of increasing C18:1PC:NTS1-B molar ratios, measured at 18 °C. The solid line shows a fit to Eq. 1 assuming that $Kr = 1$, giving a stoichiometry of 11 ± 1 lipids associated to a NTS1-B molecule ($Nb = 11 \pm 1$) at the $[(1-f/f)] = 0$ intercept. Error bars correspond to the maximum range of error introduced upon determination of the fraction of immobile component and determination of the lipid:protein molar ratio in each case.

assuming that $K_r^{PC} = 1$ it is also possible to determine the N_b value on an individual basis for each sample. Table 1 summarises the N_b values obtained applying Eq. 1 individually to each sample considering the maximum range of error introduced upon determination of the fraction of slow motion component and determination of the lipid:protein molar ratio in each case. In all cases the N_b values are close to the collective fit shown in Fig. 2. From the dimensions obtained in crystal structures it can be estimated that an annulus of about 23 lipid molecules will be necessary to fully solvate the transmembrane region of the receptor [58]. Thus, the low N_b values obtained here suggest an oligomeric state of the protein under our experimental conditions, where protein–protein contact sites reduce the number of lipid–protein contact sites.

3.3. Hydrophobic mismatch

Hydrophobic matching between the lipid bilayer and the transmembrane region of membrane proteins has been shown to influence their oligomeric or aggregation state [59]. Fig. 3 shows the ESR spectra for 14-PCSL in membranes of increasing hydrophobic thickness containing a lipid:NTS1-B molar ratio of 40:1. The spectra are very similar in C18:1PC, C20:1PC and C22:1PC membranes, whose respective hydrophobic thicknesses are 27, 30.5 and 34 Å (Table S1), as measured from the C-2 in the acyl chains of one leaflet to the C-2 in the opposite leaflet [60]. The outer peaks of the broad slower motion spectral component that arises from the population of spin-labelled lipid in contact with the protein (solid arrows) do not vary, but the outer peaks of the narrower faster motion spectral component corresponding to the spin-labelled lipid in the bulk bilayer (dashed arrows) become broader and less intense with increasing hydrophobic thickness. Deconvolution of the spectra shows that the fraction of each component does not vary significantly (Table 1), so that in all cases a similar fraction of spin-labelled lipid is in contact with the receptor. This suggests that the observed decrease in the intensity and width of the fast motion component when increasing hydrophobic thickness is due to an increase in the number of van der Waals interactions between the acyl chains, so that the motion of the spin-labelled lipid in the bulk bilayer is reduced. Because the fraction of lipid in contact with the protein is similar in all bilayers, the transmembranous protein surface available for interaction with lipids is most likely to be the same in the three membranes suggesting that the oligomeric state of the receptor does not change significantly within the studied bilayer hydrophobic thicknesses.

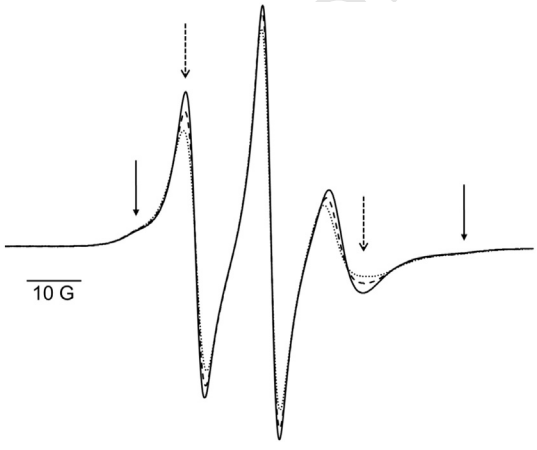

Fig. 3. Single column fitting. ESR spectra for 14-PCSL in lipid bilayers of increasing thickness containing NTS1-B at a lipid:protein molar ratio of 40:1. Solid line for C18:1PC membranes, dashed line for C20:1PC membranes and dotted line for C22:1PC membranes. Solid arrows point the outer peaks of the slow motion component while dashed arrows point to those of the fast motion component. Measurements were recorded at 25 °C, well above the phase transition temperature of the three lipid species, with a total scan width of 150 G. The spectra are normalized to equal second integrals.

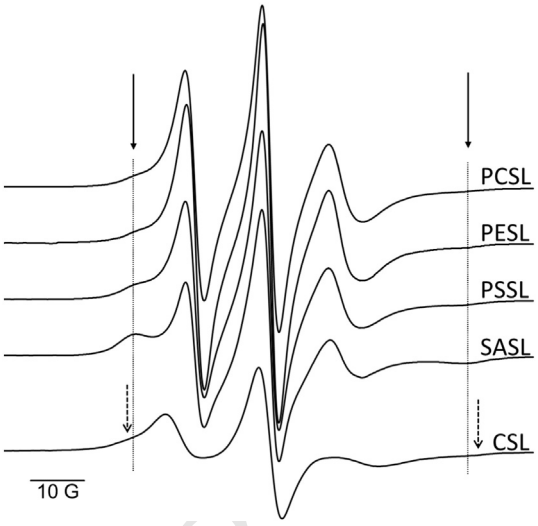

Fig. 4. Single column fitting. ESR spectra of the given spin-labelled lipid species in C18:1PC membranes containing NTS1-B at a lipid:protein molar ratio of 40:1. The outer peaks of the slow motion component are indicated by the solid arrows and vertical dotted lines except for the CSL spectrum which has a broader slow motion component indicated by the dashed arrows. Measurements were recorded at 25 °C with a total scan width of 150 G. The spectra are normalized to equal second integrals.

3.4. Relative lipid affinities for NTS1-B

Fig. 4 shows the ESR spectra for different spin-labelled lipids in C18:1PC membranes containing a lipid:NTS1-B molar ratio of 40:1. For spin-labelled lipids with higher affinity for NTS1-B the fraction of slow motion component is greater (Table 2). Comparing the fractions of slow and fast motion components of these spectra allows determining relative lipid binding constants for the protein. Because C18:1PC is the host lipid, 14-PCSL is taken as the reference spin-labelled lipid. Then, at spin-labelled lipid concentrations ($\ll N_t$), constant lipid:protein molar ratio (N_t), and assuming a similar number of lipid binding sites (N_b) for the given spin-labelled lipids, it follows from Eq. 1.

$$\left(K_r/K_r^{PC}\right) = [f(1-f_0)]/[f_0(1-f)] \quad (2)$$

where f_0 is the fraction of slow motion 14-PCSL in C18:1PC, and K_r^{PC} is the binding constant of 14-PCSL relative to C18:1PC [42,45]. Assuming that 14-PCSL has no selectivity for the protein relative to the host lipid C18:1PC ($K_r^{PC} = 1$), Eq. 2 directly gives the relative binding constant K_r of the other spin-labelled lipids relative to C18:1PC. The f and K_r values derived from the spectra in Fig. 4 are summarised in Table 2. The anionic lipids 14-PSSL and 14-SASL bind, respectively, with two and five times greater affinity for the receptor compared to PC, while uncharged PESL and CSL show no relative selectivity for the protein.

Table 2
Fraction of the slow motion component and lipid binding constants relative to C18:1PC (K_r) derived from the ESR spectra from 14-PCSL, 14-PESL, 14-PSSL, 14-SASL and CSL in C18:1PC membranes containing NTS1-B at a lipid:protein molar ratio of 40:1 (spectra from Fig. 4). The error is the maximum range of error introduced upon determination of the fraction of immobile component (f). The error for the K_r values is the maximum difference between the K_r value and the value obtained when K_r is calculated taking the extreme error values for f.

Spin-labelled lipid	Fraction of slow motion component (f)	Binding constant relative to C18:1PC (K_r / K_r^{PC})
14-PCSL	0.29 ± 0.01	1.00
14-PESL	0.30 ± 0.01	1.05 ± 0.05
14-PSSL	0.44 ± 0.01	1.92 ± 0.08
14-SASL	0.68 ± 0.02	5.20 ± 0.51
CSL	0.27 ± 0.04	0.91 ± 0.19

3.5. Molecular dynamics simulations

In order to gain detailed insights about specific NTS1–lipid interactions that could aid in understanding the different lipid affinities derived from ESR experiments, atomistic (AT) MD simulations were carried out for a NTS1 model based on the crystal structure of PDB ID: 4BUO [50]. R305, the only mutated charged residue in this structure which is accessible to lipid molecules, was back-mutated to the wild type H305 to avoid the possible appearance of "artificial" clusters of PS lipids around this point mutation. Simulations were performed in bilayers resembling the composition of brain polar lipid extract (Avanti) because this lipid mixture has been shown to optimally support ligand binding of NTS1 [40] and contains the main lipids found in mammalian plasma membranes also studied here with ESR. The calculated average thickness value for the simulated BPL-like model membrane was 41.8 ± 0.4 Å (phosphorus to phosphorous distance), therefore very similar to the experimental thickness reported for a C20:1PC lipid bilayer (Table S1, [60]). The average number of contacts with each type of lipid within a radius of 4 Å from the protein was very similar for PC, PE, and cholesterol, while for PS it was about double that of the other lipids (Fig. 5A). This is in very good agreement with the relative affinities derived by ESR (almost identical for PC and PE, and nearly double for PS binding to NTS1, Table 2). The MD simulation also indicated different lipid preferences for the extracellular (EC) and intracellular (IC) sides of NTS1. In particular, PC and PS showed higher relative frequency of contacts for the EC and IC domains, respectively (Fig. 5A), while cholesterol and PE presented very similar contacts with both domains. This observation correlates well with the fact that the majority of PS lipid molecules are located in the IC side of the mammalian plasma membrane and PC molecules are more abundant in the extracellular side [61]. Interactions of PS with lipid-exposed positively charged residues (see discussion) were studied using the same criteria. Preferential contacts to $R185^{4.41}$ were observed, followed by $K188^{4.44}$, $R377^{8.51}$ $K263^{5.64}$, $R304^{6.31}$ and $R311^{6.38}$ (Fig. 5B). Thus, the IC end of TM4 and TM6 may represent high affinity binding sites for PS (Fig. S3).

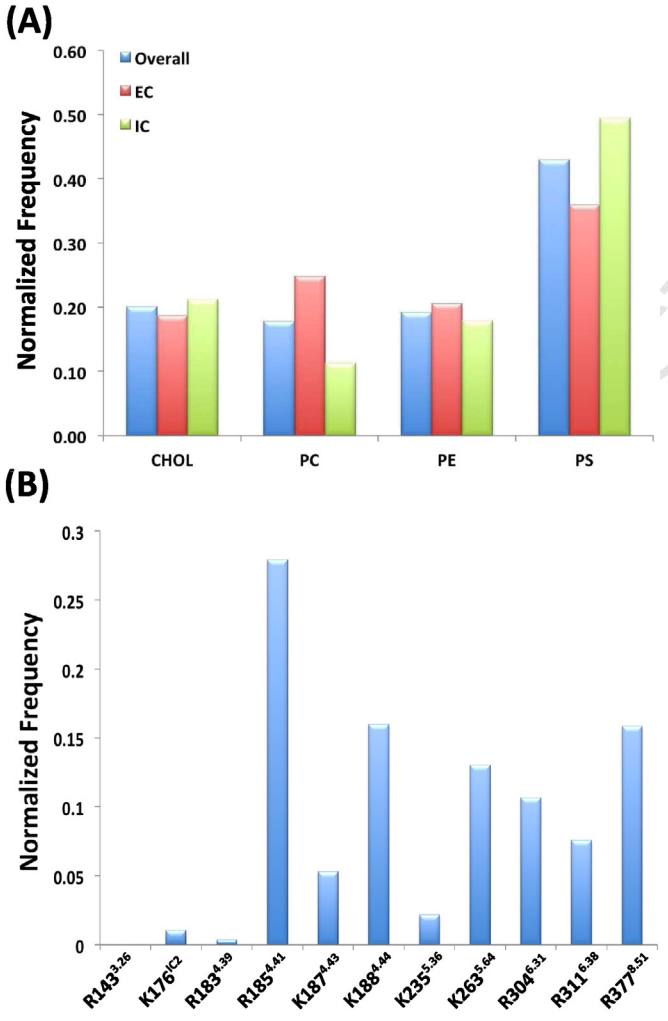

Fig. 5. Single column fitting. (A) Normalized frequency of specific lipid interactions with the extracellular (red bars), intracellular (green bars), and both (blue bars) domains of NTS1. The number of contacts was normalized against the fraction of each lipid in the membrane. (B) Per-residue normalized frequency of specific PS headgroup interactions with the positively charged amino acids of NTS1 that are exposed to the lipid bilayer. In (A) and (B) data was obtained over 180 ns of MD simulation (20–200 ns fragment) of H305R backmutated NTS1 structure (PDB ID: 4BUO) modelled within a BPL-like membrane.

4. Discussion

4.1. Stoichiometry of NTS1-B and associated lipid molecules

At lipid:NTS1-B molar ratios ranging from 40:1 to 80:1 the fraction of slow motion 14-PCSL indicates a constant and low number of associated lipid molecules to each receptor molecule ($N_b = 11 \pm 1$, assuming that $K_r^{PC} = 1$). Similar studies for frog [62] and bovine [17] rhodopsin in their native rod outer disc membranes gave N_b values of 22 ± 2 and 24 ± 3, respectively, where the native membrane lipid:rhodopsin molar ratio is of 61:1. Bovine rhodopsin reconstituted at a lipid:rhodopsin molar ratio of 60:1 in C14:0PC or C15:0PC bilayers also gave an N_b value of ca. 22 [63]. The values reported for rhodopsin coincide with the number of lipid molecules that would be required to solvate the perimeter of the seven transmembrane domain receptor, as evidenced from modelling of lipid molecules around the crystal structure of rhodopsin [58]. Numerous similar ESR studies have given N_b values for other membrane proteins that also match those expected from crystal structures [58]. The low N_b value of 11 ± 1 reported here for NTS1-B thus implies that protein–protein contacts occur reducing the surface of the receptor available for interaction with lipid molecules [64]. Previously, using fluorescence energy transfer in NTS1 fused to fluorescent proteins, we described constitutive dimerisation of the receptor at higher lipid:protein molar ratios from ~600:1 to ~1000:1 when reconstituted into bilayers from porcine brain polar lipid extract [10], and later we showed that the degree of dimerisation, as reported by FRET efficiency, is affected by the specific lipid composition of the bilayer [40]. In C16:0–C18:1PC membranes FRET efficiency was low compared to that in BPL membranes [40], so that in our present study in C18:1PC membranes we would expect little dimerisation, although potential effects due to difference in the lipid acyl chain saturation were not explored. However, an important difference with respect the FRET study is the lipid:protein molar ratio, with molar ratios ranging from 40:1 to 80:1 of lipid to protein in our ESR experiments, the higher protein concentration could favour dimerisation in PC membranes. This is also in good agreement with a study showing concentration dependent dimerisation of rat NTS1 in detergent micelles [65].

The current experiments in our laboratory in which we measure distances between the monomers of a dimer using small fluorescence or spin label probes attached at particular transmembrane helices of NTS1, suggest that association of receptors can occur dynamically through interfaces involving different helices (unpublished). An NTS1 dimer model derived from our ongoing experiments indicate that, for a receptor molecule, the accessible surface to the lipid bilayer decreases by about 23% in a dimer compared to that of a monomer (unpublished). However, the N_b value measured for NTS1-B here is about half of that expected for a monomer, which would imply a 50% decrease in lipid accessible surface per receptor molecule, thus suggesting a higher order oligomeric arrangement in the present study. The 'promiscuity' of receptor–receptor interface associations observed in our unpublished experiments could explain why at the lower lipid:protein molar ratios

higher oligomeric arrangements occur. This promiscuity of associations makes it very difficult to infer the stoichiometry of the oligomers from the N_b value, because the surface area accessible to the lipid bilayer varies depending on the particular protein–protein interface.

The low N_b value does not arise from random protein–protein contacts at the low lipid:protein molar ratios studied here because the probability of protein–protein contacts is still very low at these molar ratios [46] as evidenced for rhodopsin and numerous other membrane proteins studied this way [45]. Furthermore, random protein–protein contacts would decrease upon increasing lipid:protein molar ratio, and here this is not the case as N_b remains constant from 40:1 to 80:1 lipid:protein molar ratios (Table 1). For this reason, nonspecific aggregation of the receptor is also unlikely. In contrast, a recent study combining ESR and fluorescence experiments showed aggregation of the bacterial potassium channel KcsA at lipid:channel molar ratios ranging from 30:1 to 75:1. The N_b values for KcsA at these molar ratios increased when decreasing protein concentration and were lower than the number of lipids necessary to fully solvate the transmembranous region of the channel. However, at higher molar ratios the channel did not aggregate: the N_b value was constant and coincided with the number of lipids required to cover the perimeter of the channel [66].

Finally, it must be considered that it is impossible to discard any influence of the fusion partners on oligomerisation. However, both MBP and Trx are used widely to aid maintaining the biological function of heterologously expressed proteins and are not expected to drive artefactual aggregation/oligomerisation. On the other hand, stearic hindrance could limit receptor–receptor interactions, but this seems not to be the case given the consistent, low N_b value.

4.2. Effect of increasing the thickness of the lipid bilayer

Hydrophobic matching between the lipid bilayer and the hydrophobic segment of transmembrane proteins is important, and there are a number of ways to compensate the energy cost of hydrophobic mismatch which can affect protein function [59]. ESR studies of the type reported here with spin-labelled lipids in combination with saturation transfer experiments of spin-labelled bovine rhodopsin showed that varying the hydrophobic thickness of the bilayer could induce extensive aggregation or an oligomeric arrangement of the receptor [63,67]. More recently, FRET studies with Alexa fluorophores attached to bovine rhodopsin also showed a dependence of receptor oligomerisation/aggregation on lipid chain length [68]. Comparing the choice of saturated or monounsaturated PC lipids, and the different lipid:rhodopsin molar ratios used in the aforementioned studies also reveals that these factors can influence rhodopsin oligomerisation/aggregation. Polyunsaturated acyl chains have been shown to interact more favourably with rhodopsin than saturated chains [69], so that it is not surprising that unsaturation and hydrophobic thickness can together influence the aggregation/oligomeric state of the receptor.

In the current work, the lipid of choice was C18:1PC, as described above, which has a bilayer phosphate–phosphate distance 4.5 Å shorter than the average mammalian plasma membrane (Table S1). We also reconstituted the receptor in thicker bilayers (Fig. 3), the C20:1PC and C22:1PC membranes having phosphate–phosphate distances of 41.5 and 45.0 Å respectively, but we observed no change in the N_b values for NTS1-B. This suggests that the oligomeric state of the receptor is stable across this short range of hydrophobic thicknesses, which covers the range of thicknesses of membranes found in the exocytic pathway of rat liver cells (Table S1, to our knowledge, the only mammalian cells for which bilayer thicknesses have been measured directly [70]). The stability in the oligomeric arrangement suggests that the bilayer accommodates to the hydrophobic thickness of the oligomeric protein, rather than any alteration in the protein folding to match the hydrophobic thickness of the bilayer, which would be expected to affect oligomerisation.

4.3. Relative lipid affinities for NTS1-B

We measured the relative lipid affinities for NTS1-B of lipid species that are major components of the mammalian plasma membrane (Table 2). It is important to keep in mind that these interactions are for oligomeric NTS1-B, where some lipid binding sites in the monomeric form can be occluded, while new sites can be generated at the protein–protein interfaces. Both PC and PE, showed no relative selectivity for the receptor. We have previously reported that for NTS1 in reconstituted systems, the presence of PE as a major component of the lipid bilayer is important for effective binding of neurotensin [40]. Since PE shows little relative affinity for NTS1, one possibility is that this lipid exerts a bulk collective effect on the receptor. On the other hand, because PE is abundant in the bilayer, binding at a specific site to modulate function could not require high affinity for the lipid, because there would be sufficient lipid molecules around to interact with such a site, and therefore it is difficult to suggest a mechanism by which PE could mediate its effects on NTS1. For example, using ESR and spin-labelled lipids with bovine rhodopsin did not show selectivity for the PE headgroup [17], but recent studies have suggested that a combination of the collective effect of PE on the physical properties of the bilayer together with the level of acyl chain unsaturation and the ability of PE to engage in direct, water-free hydrogen bonding [71] with the protein are important to influence receptor function [72].

Negatively charged PS is the third most abundant of the phosphoglycerolipids in plasma membrane after PC and PE [56]. PS showed approximately double the affinity for the receptor compared to zwitterionic PC and PE, while the negatively charged fatty acid showed ca. five times the affinity compared to that of the zwitterionic lipids. The differences in affinity could, in principle, be due to exposed positively charged residues at the lipid headgroup region of the bilayer. Crystal structures of stabilised mutants of NTS1 show positively charged residues that could interact with lipid headgroups in the bilayer, and which are native to the NTS1 sequence (Fig. 6, from PDB ID: 4BUO [50]). In the structure from White et al. [73] (PDB ID: 4GRV), although not all side chains have been resolved, R304$^{6.31}$ and R311$^{6.38}$ in transmembrane helix 6 (TM6) appear in close proximity constituting a potential high affinity binding site for negatively charged phospholipids at the IC side. In the 4BUO structure [50], all of the positively charged side chains expected to be facing the lipid bilayer are resolved and are scattered around what would be the lipid-water interface, with a group of three close positively charged residues (R185$^{4.41}$, K187$^{4.43}$

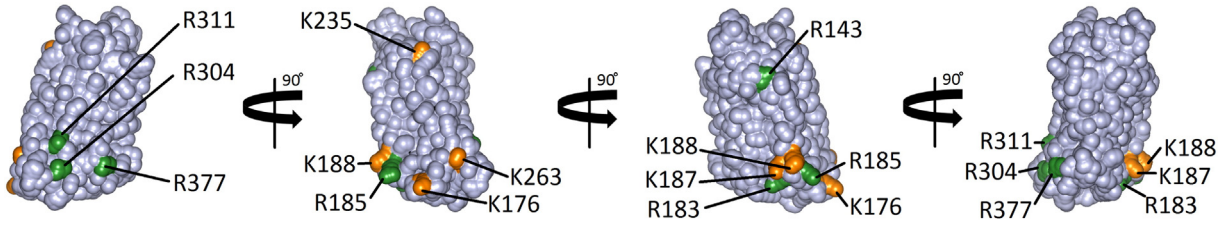

Fig. 6. 2-Column fitting. Solvent accessible surface of NTS1 (PDB ID: 4BUO). Lysine and arginine residues that could interact with lipids in the bilayer are coloured orange and green, respectively. Images generated with The PyMol Molecular Graphics System, Version 1.7.0.5 Schrödinger, LLC.

Please cite this article as: J.H. Bolivar, et al., Interaction of lipids with the neurotensin receptor 1, Biochim. Biophys. Acta (2016), http://dx.doi.org/10.1016/j.bbamem.2016.02.032

and K188$^{4.44}$), at the IC side of TM4 (Fig. 6). The chains of the R304$^{6.31}$ and R311$^{6.38}$ residues in TM6 in the 4BUO structure are, however, pointing further apart than in the 4GRV structure. The IC side of TM6 is one of the regions of the receptor where the two structures differ most, probably due to the absence of the interfacial helix 8 in 4GRV, which has been proposed to result in a displacement of TM6 towards an "active-like" position [50]. Movement of TM6 is critical for signal transduction and G protein coupling [74], and it has been shown that for the β_2-adrenergic receptor (β_2AR) TM6 is highly dynamic, sampling several conformational states with and, to a lesser extent, without bound agonist [75,76]. Therefore, lipids interacting with TM6 could influence its conformational state, having an impact on G protein coupling. It is attractive to speculate that different conformational states could expose/hide lipid binding sites through which lipids could exert their modulatory effects. Remarkably, recent MD simulations on β_2AR show that the space exposed by the movement of TM6 in the active structures allows penetration of lipid molecules which interact with R3.50 and stabilise the active conformation, with anionic lipids binding more frequently [77]. Experimental evidence correlating direct measurement of lipid interactions with channel opening has been obtained for the mechanosensitive channel MscL [78–80] and the potassium channel KcsA [81]. In this case, Lee and co-workers measured relative lipid binding constants by quenching Trp fluorescence with lipids brominated at the acyl chains [82]. In the case of MscL, by placing a single Trp residue at a site close to a cluster of positively charged residues they were able to measure relative lipid affinities for a single high affinity lipid binding site on the protein. The measurements gave PS and phosphatidic acid (PA) binding constants relative to PC of 5.0 ± 0.6 and 8.4 ± 0.5 [78]. Later they showed that interaction with negatively charged lipids modulates channel opening [79] and that such modulation is mediated by binding of the negatively charged lipids at the cluster of positively charged residues [80]. The relative lipid binding constants in MscL reported by Powl et al. for PS and PA are significantly higher than that obtained here for PS using ESR. However, two important things must be considered. First, the distribution of PS in the mammalian plasma membrane is asymmetric [61], with the majority being located in the IC side. This means that the fraction of PS constituting the inner leaflet is very high, so that binding at a particular site on a protein at the IC side will not require very high affinity binding sites. Second, the binding constants reported by Powl et al. [78] were determined for a specific site, while the binding constants reported by the ESR method are a weighted average for all the lipid binding sites in the protein [42,45,57], so that the binding constant for a high affinity binding site is averaged together with the binding constants for lower affinity binding sites. This means that it is perfectly reasonable to suggest a role for PS in modulating receptor function through direct interaction. Our MD simulation of the NTS1 monomer in the BPL-like membrane is in agreement with the ESR data, and points to specific high affinity sites in the IC side of TM4 and TM6 where PS could bind to exert modulatory effects (Fig. 5B and Fig. S3); mutating these residues will be important to determine their role in the interaction with lipids and potential receptor function modulation. Other residues that could become accessible to the lipid bilayer upon receptor activation, as observed for the β_2AR [77], must also be considered.

The relative binding constant obtained here for the fatty acid (K_r = 5.20 ± 0.51) is much higher than for PC, PE, or PS. A possible explanation for this higher affinity could be that the smaller headgroup of the fatty acid allows easier access to crevices of the protein. It is expected that the negative charge in the fatty acid will also be important, although fatty acids incorporated into lipid bilayers have their pK_a shifted towards physiological pH, so only roughly 40% of the fatty acid is expected to be deprotonated [83]. Nonetheless, the microenvironment provided by a positively charged cluster of residues could affect this pK_a to favour deprotonation of the fatty acid, strengthening the interaction at such site. Fatty acids, in particular polyunsaturated fatty acids, are well known for acting as signalling molecules that are able to affect the activity of a wide range of ion channels [84,85]. These messenger molecules are released upon stimuli through phospholipases, and recently have been shown to be able to modulate the activity of potassium channels (in vitro and in celulla) through direct binding at the pore of these channels [86,87]. Using ESR [88] and fluorescence [89] with spin-labelled and fluorescently labelled fatty acids, respectively, it has been possible to measure directly binding constants for fatty acids to the pore of a potassium channel. NTS1 has been shown to mediate release of arachidonic acid through G protein activation [90], therefore, an interesting possibility arises that fatty acids could also have a modulatory effect on NTS1 and other GPCRs through direct interactions upon local release from cellular stimuli. The recent crystal structure of the A_{2A} adenosine receptor obtained from lipid cubic phase showed numerous associated lipid chains whose headgroups were not resolved [91]. Some of these lipid chains, most of them modelled as oleic acid, were intimately associated with the receptor, one of them protruding into the ligand binding pocket, providing structural insights into potential modes of interaction of fatty acids with a GPCR.

The spin-labelled cholesterol analogue, CSL, showed no relative selectivity for NTS1-B. A large number of studies document the importance of cholesterol for GPRC function (discussed in refs. [1–3]). For rhodopsin, cholesterol has been shown to influence receptor function and stability [92–94], but no selectivity for CSL relative to PC was observed using ESR studies of the type presented here, assuming similar binding sites for both lipids [17]. The latter ESR study did show, however, that CSL is able to interact with rhodopsin, in agreement with later FRET experiments between Trp (donor) and the cholesterol analogue cholestatrienol (acceptor) [18]. The FRET study further revealed that cholestatrienol–rhodopsin interactions could be displaced by cholesterol but not by ergosterol, suggesting specific binding sites for cholesterol. In the case of the serotonin$_{1A}$ receptor, experiments with cholesterol stereoisomers have suggested a stereospecific interaction of cholesterol with the receptor affect agonist binding, although effects due to changes in the bulk physical properties of the bilayer could not be discarded [95]. Cholesterol also has some influence on NTS1; we showed that it can affect receptor oligomerisation and that the analogue CHS increases the stability of the receptor to some extent [40], however, NTS1 is capable of ligand binding and G protein coupling in the absence of cholesterol [12,15,40,55]. The conserved cholesterol motive (CCM) proposed as a site for interaction of cholesterol with GPCRs [96] and a more generic CRAC motif (cholesterol recognition/interaction amino acid consensus, identified first in other membrane proteins [97] and later in GPCRs [98]) are found in the NTS1 sequence [40], but whether cholesterol influences NTS1 through direct interaction with these motives remains unknown. The broad component in Fig. 4 for CSL shows that, although this analogue does not have higher affinity for NTS1-B relative to PC, it is able to interact with the receptor, so that binding at the proposed cholesterol motives cannot be ruled out. Fluorescence experiments of the type performed with rhodopsin in combination with site directed mutagenesis could be a good way to explore this possibility.

Finally, it is important to note that the relative lipid binding constants determined here are for a small fraction of spin-labelled lipid (1 mol%) in the C18:1PC background, so that the spin-labelled lipids cannot affect the bulk biophysical properties of the bilayer. This means that the relative affinities measured rely on the ability of the different lipid species to establish interactions with the receptor in the 18:1PC membrane background. Generally, it is very difficult to determine whether the effects of lipids on membrane proteins are due to the bulk physical properties of the bilayer or due to interactions between particular lipids and particular sites [99]. The experiments presented here therefore offer a unique opportunity to measure lipid–receptor interactions without the influence of bulk physical effects, and will be critical for future interpretation of the important functional dependence of NTS1 and other GPCRs on lipids.

Numerous studies have shown the lipid environment is critical for rhodopsin function, and it is becoming evident that the same holds for

Please cite this article as: J.H. Bolivar, et al., Interaction of lipids with the neurotensin receptor 1, Biochim. Biophys. Acta (2016), http://dx.doi.org/10.1016/j.bbamem.2016.02.032

NTS1 and other GPRCs. However, as our knowledge on other GPCRs increases, it is apparent that despite marked similarities between the crystal structures of rhodopsin and other GPCRs, there are important differences in receptor dynamics [100]. Lipids can affect receptor dynamics [20], and here we show that the way lipids interact with NTS1 is also very different to the way lipids interact with rhodopsin. Membrane proteins have co-evolved with the lipid composition of the membranes surrounding them, and for such a diverse and versatile group of proteins as GPCRs it is reasonable to think that evolution has fine-tuned receptor function to its membrane environment. Much effort will be necessary to dissect all the factors that affect GPCRs and to understand how all these factors orchestrate GPCR biological function in vivo.

Transparency document

The Transparency document associated with this article can be found, in the online version.

Acknowledgements

Funding was provided by the Medical Research Council (MRC) (Grant no. G0900076 to AW). ESR measurements were performed at the Centre for Advance Electron Spin Resonance (CAESR), supported by the Engineering and Physical Sciences Research Council (EPSRC), (EP/D048559/1), AW co-applicant. MD simulations were run on a cluster in the Structural Bioinformatics & Computational Biochemistry unit (Dept. Biochemistry, University of Oxford; http://sbcb.bioch.ox.ac.uk/), and on the Emerald GPU cluster (https://www.emerald.rl.ac.uk//).

References

[1] Y. Paila, A. Chattopadhyay, Membrane cholesterol in the function and organization of G-protein coupled receptors, in: J.R. Harris (Ed.) Cholesterol Binding and Cholesterol Transport Proteins: Structure and Function in Health and Disease, 51, Springer Science and Business Media 2010, pp. 439–466.
[2] B. Chini, M. Parenti, G-protein-coupled receptors, cholesterol and palmitoylation: facts about fats, J. Mol. Endocrinol. 42 (2009) 371–379.
[3] J. Oates, A. Watts, Uncovering the intimate relationship between lipids, cholesterol and GPCR activation, Curr. Opin. Struct. Biol. 21 (2011) 802–807.
[4] A. Chattopadhyay, GPCRs: lipid-dependent membrane receptors that act as drug targets, Adv.Biol. (2014) (2014) Article ID 143023.
[5] H. Attrill, P.J. Harding, E. Smith, S. Ross, A. Watts, Improved yield of a ligand-binding GPCR expressed in *E. coli* for structural studies, Protein Expr. Purif. 64 (2009) 32–38.
[6] S. Xiao, J.F. White, M.J. Betenbaugh, R. Grisshammer, J. Shiloach, Transient and stable expression of the neurotensin receptor NTS1: a comparison of the baculovirus-insect cell and the T-REx-293 expression systems, PLoS One 8 (2013), e63679.
[7] J.F. White, L.B. Trinh, J. Shiloach, R. Grisshammer, Automated large-scale purification of a G protein-coupled receptor for neurotensin, FEBS Lett. 564 (2004) 289–293.
[8] R. Grisshammer, P. Averbeck, A.K. Sohal, Improved purification of a rat neurotensin receptor expressed in *Escherichia coli*, Biochem. Soc. Trans. 27 (1999) 899–903.
[9] R. Grisshammer, Chapter 36 — Purification of Recombinant G-protein-coupled Receptors, in: R.B. Richard, P.D. Murray (Eds.), Methods in Enzymology, 463, Academic Press 2009, pp. 631–645.
[10] P.J. Harding, H. Attrill, J. Boehringer, S. Ross, G.H. Wadhams, E. Smith, J.P. Armitage, A. Watts, Constitutive dimerization of the G-protein coupled receptor, neurotensin receptor 1, reconstituted into phospholipid bilayers, Biophys. J. 96 (2009) 964–973.
[11] A.D. Goddard, P.M. Dijkman, R.J. Adamson, A. Watts, Chapter 18 — Lipid-dependent GPCR Dimerization, in: P.M. Conn (Ed.) Methods in Cell Biology, 117, Academic Press 2013, pp. 341–357.
[12] S. Inagaki, R. Ghirlando, J.F. White, J. Gvozdenovic-Jeremic, J.K. Northup, R. Grisshammer, Modulation of the interaction between neurotensin receptor NTS1 and Gq protein by lipid, J. Mol. Biol. 417 (2012) 95–111.
[13] E. Serebryany, G.A. Zhu, E.C.Y. Yan, Artificial membrane-like environments for in vitro studies of purified G-protein coupled receptors, Biochim. Biophys. Acta 1818 (2012) 225–233.
[14] S. Luca, J.F. White, A.K. Sohal, D.V. Filippov, J.H. van Boom, R. Grisshammer, M. Baldus, The conformation of neurotensin bound to its G protein-coupled receptor, Proc. Natl. Acad. Sci. U. S. A. 100 (2003) 10706–10711.
[15] R.J. Adamson, A. Watts, Kinetics of the early events of GPCR signalling, FEBS Lett. 588 (2014) 4701–4707.
[16] A.D. Goddard, P.M. Dijkman, R.J. Adamson, R.I. dos Reis, A. Watts, Chapter 19 — Reconstitution of Membrane Proteins: A GPCR as An Example, in: K.S. Arun (Ed.) Methods in Enzymology, 556, Academic Press 2015, pp. 405–424.
[17] A. Watts, I.D. Volotovski, D. Marsh, Rhodopsin–lipid associations in bovine rod outer segment membranes. Identification of immobilized lipid by spin-labels, Biochemistry 18 (1979) 5006–5013.
[18] A.D. Albert, J.E. Young, P.L. Yeagle, Rhodopsin–cholesterol interactions in bovine rod outer segment disk membranes, Biochim. Biophys. Acta 1285 (1996) 47–55.
[19] O. Soubias, W.E. Teague, K. Gawrisch, Evidence for specificity in lipid–rhodopsin interactions, J. Biol. Chem. 281 (2006) 33233–33241.
[20] O. Soubias, K. Gawrisch, The role of the lipid matrix for structure and function of the GPCR rhodopsin, Biochim. Biophys. Acta 1818 (2012) 234–240.
[21] M. Numao, H. Sudo, I. Yamamoto, N. Nakao, H. Kaiya, M. Miyazato, N. Tsushima, M. Tanaka, Molecular characterization of structure and tissue distribution of chicken neurotensin receptor, Gen. Comp. Endocrinol. 171 (2011) 33–38.
[22] J.-I. Hwang, D.-K. Kim, H.B. Kwon, H. Vaudry, J.Y. Seong, Phylogenetic history, pharmacological features, and signal transduction of neurotensin receptors in vertebrates, Ann. N. Y. Acad. Sci. 1163 (2009) 169–178.
[23] K. Tanaka, M. Masu, S. Nakanishi, Structure and functional expression of the cloned rat neurotensin receptor, Neuron 4 (1990) 847–854.
[24] E. Moyse, W. Rostène, M. Vial, K. Leonard, J. Mazella, P. Kitabgi, J.P. Vincent, A. Beaudet, Distribution of neurotensin binding sites in rat brain: a light microscopic radioautographic study using monoiodo [125I]Tyr3-neurotensin, Neuroscience 22 (1987) 525–536.
[25] R. Elde, M. Schalling, S. Ceccatelli, S. Nakanishi, T. Hökfelt, Localization of neuropeptide receptor mRNA in rat brain: initial observations using probes for neurotensin and substance P receptors, Neurosci. Lett. 120 (1990) 134–138.
[26] H. Boudin, D. Pélaprat, W. Rostène, A. Beaudet, Cellular distribution of neurotensin receptors in rat brain: immunohistochemical study using an antipeptide antibody against the cloned high affinity receptor, J. Comp. Neurol. 373 (1996) 76–89.
[27] X. Zhang, Z.Q. Xu, L. Bao, Å. Dagerlind, T. Hökfelt, Complementary distribution of receptors for neurotensin and NPY in small neurons in rat lumbar DRGs and regulation of the receptors and peptides after peripheral …, J. Neurosci. 15 (1995) 2733–2747.
[28] N. Vita, P. Laurent, S. Lefort, P. Chalon, X. Dumont, M. Kaghad, D. Gully, G. Le Fur, P. Ferrara, D. Caput, Cloning and expression of a complementary DNA encoding a high affinity human neurotensin receptor, FEBS Lett. 317 (1993) 139–142.
[29] R. Cáceda, B. Kinkead, C.B. Nemeroff, Neurotensin: role in psychiatric and neurological diseases, Peptides 27 (2006) 2385–2404.
[30] S. Dupouy, N. Mourra, V.K. Doan, A. Gompel, M. Alifano, P. Forgez, The potential use of the neurotensin high affinity receptor 1 as a biomarker for cancer progression and as a component of personalized medicine in selective cancers, Biochimie 93 (2011) 1369–1378.
[31] Z. Wu, D. Martinez-Fong, J. Trédaniel, P. Forgez, Neurotensin and its high affinity receptor 1 as a potential pharmacological target in cancer therapy, Front. Endocrinol. 3 (2013).
[32] M. Yamada, M. Yamada, M.A. Watson, E. Richelson, Deletion mutation in the putative third intracellular loop of the rat neurotensin receptor abolishes polyphosphoinositide hydrolysis but not cyclic AMP formation in CHO-K1 cells, Mol. Pharmacol. 46 (1994) 470–476.
[33] M. Najimi, P. Gailly, J.-M. Maloteaux, E. Hermans, Distinct regions of C-terminus of the high affinity neurotensin receptor mediate the functional coupling with pertussis toxin sensitive and insensitive G-proteins, FEBS Lett. 512 (2002) 329–333.
[34] D. Skrzydelski, A.-M. Lhiaubet, A. Lebeau, P. Forgez, M. Yamada, E. Hermans, W. Rostene, D. Pelaprat, Differential involvement of intracellular domains of the rat NTS1 neurotensin receptor in coupling to G proteins: a molecular basis for agonist-directed trafficking of receptor stimulus, Mol. Pharmacol. 64 (2003) 421–429.
[35] M. Hillenbrand, C. Schori, J. Schöppe, A. Plückthun, Comprehensive analysis of heterotrimeric G-protein complex diversity and their interactions with GPCRs in solution, Proc. Natl. Acad. Sci. U. S. A. 112 (2015) E1181–E1190.
[36] D. Pelaprat, Interactions between neurotensin receptors and G proteins, Peptides 27 (2006) 2476–2487.
[37] B. Bai, X. Cai, Y. Jiang, E. Karteris, J. Chen, Heterodimerization of apelin receptor and neurotensin receptor 1 induces phosphorylation of ERK1/2 and cell proliferation via Gαq-mediated mechanism, J. Cell. Mol. Med. 18 (2014) 2071–2081.
[38] J.R. Hwang, M.W. Baek, J. Sim, H.-S. Choi, J.M. Han, Y.L. Kim, J.-I. Hwang, H.B. Kwon, N. Beaudet, P. Sarret, J.Y. Seong, Intermolecular cross-talk between NTR1 and NTR2 neurotensin receptor promotes intracellular sequestration and functional inhibition of NTR1 receptors, Biochem. Biophys. Res. Commun. 391 (2010) 1007–1013.
[39] A. Goddard, A. Watts, Regulation of G protein-coupled receptors by palmitoylation and cholesterol, BMC Biol. 10 (2012) 27.
[40] J. Oates, B. Faust, H. Attrill, P. Harding, M. Orwick, A. Watts, The role of cholesterol on the activity and stability of neurotensin receptor 1, Biochim. Biophys. Acta 1818 (2012) 2228–2233.
[41] P.M. Dijkman, A. Watts, Lipid modulation of early G protein-coupled receptor signalling events, Biochim. Biophys. Acta 1848 (2015) 2889–2897.
[42] D. Marsh, A. Watts, Spin Labeling and Lipid–Protein Interactions in Membranes, in: P.C. Jost, O.H. Griffith (Eds.), Lipid–Protein Interactions, 2, Wiley-Interscience, New York - Brisbane - Chichester - Toronto, 1982.
[43] C.N. Pace, F. Vajdos, L. Fee, G. Grimsley, T. Gray, How to measure and predict the molar absorption coefficient of a protein, Protein Sci. 4 (1995) 2411–2423.
[44] P. Artimo, M. Jonnalagedda, K. Arnold, D. Baratin, G. Csardi, E. de Castro, S. Duvaud, V. Flegel, A. Fortier, E. Gasteiger, A. Grosdidier, C. Hernandez, V. Ioannidis, D. Kuznetsov, R. Liechti, S. Moretti, K. Mostaguir, N. Redaschi, G. Rossier, I. Xenarios, H. Stockinger, ExPASy: SIB bioinformatics resource portal, Nucleic Acids Res. 40 (2012) W597–W603.

Please cite this article as: J.H. Bolivar, et al., Interaction of lipids with the neurotensin receptor 1, Biochim. Biophys. Acta (2016), http://dx.doi.org/10.1016/j.bbamem.2016.02.032

[45] D. Marsh, Electron spin resonance in membrane research: protein–lipid interactions, Methods 46 (2008) 83–96.
[46] J.M. East, D. Melville, A.G. Lee, Exchange rates and numbers of annular lipids for the calcium and magnesium ion dependent adenosine triphosphatase, Biochemistry 24 (1985) 2615–2623.
[47] B. Hess, C. Kutzner, D. van der Spoel, E. Lindahl, GROMACS 4: algorithms for highly efficient, load-balanced, and scalable molecular simulation, J. Chem. Theory Comput. 4 (2008) 435–447.
[48] Phillip J. Stansfeld, Joseph E. Goose, M. Caffrey, Elisabeth P. Carpenter, Joanne L. Parker, S. Newstead, Mark S.P. Sansom, MemProtMD: automated insertion of membrane protein structures into explicit lipid membranes, Structure 23 (2015) 1350–1361.
[49] H.J.C. Berendsen, J.P.M. Postma, W.F. van Gunsteren, J. Hermans, Interaction Models for Water in Relation to Protein Hydration, in: B. Pullman (Ed.) Intermolecular Forces, 14, Springer Netherlands 1981, pp. 331–342.
[50] P. Egloff, M. Hillenbrand, C. Klenk, A. Batyuk, P. Heine, S. Balada, K.M. Schlinkmann, D.J. Scott, M. Schütz, A. Plückthun, Structure of signaling-competent neurotensin receptor 1 obtained by directed evolution in *Escherichia coli*, Proc. Natl. Acad. Sci. U. S. A. 111 (2014) E655–E662.
[51] A. Šali, T.L. Blundell, Comparative protein modelling by satisfaction of spatial restraints, J. Mol. Biol. 234 (1993) 779–815.
[52] H. Koldsø, D. Shorthouse, J. Hélie, M.S.P. Sansom, Lipid clustering correlates with membrane curvature as revealed by molecular simulations of complex lipid bilayers, PLoS Comput. Biol. 10 (2014), e1003911.
[53] P.J. Stansfeld, M.S.P. Sansom, From coarse grained to atomistic: a serial multiscale approach to membrane protein simulations, J. Chem. Theory Comput. 7 (2011) 1157–1166.
[54] C. Oostenbrink, A. Villa, A.E. Mark, W.F. Van Gunsteren, A biomolecular force field based on the free enthalpy of hydration and solvation: the GROMOS force-field parameter sets 53A5 and 53A6, J. Comput. Chem. 25 (2004) 1656–1676.
[55] R. Grisshammer, E. Hermans, Functional coupling with $G_{\alpha q}$ and $G_{\alpha i1}$ protein subunits promotes high-affinity agonist binding to the neurotensin receptor NTS-1 expressed in *Escherichia coli*, FEBS Lett. 493 (2001) 101–105.
[56] G. van Meer, D.R. Voelker, G.W. Feigenson, Membrane lipids: where they are and how they behave, Nat. Rev. Mol. Cell Biol. 9 (2008) 112–124.
[57] D. Marsh, L.I. Horvath, Structure, dynamics and composition of the lipid–protein interface. Perspectives from spin-labelling, Biochim. Biophys. Acta 1376 (1998) 267–296.
[58] T. Pali, D. Bashtovyy, D. Marsh, Stoichiometry of lipid interactions with transmembrane proteins — deduced from the 3D structures, Protein Sci. 15 (2006) 1153–1161.
[59] J.A. Killian, Hydrophobic mismatch between proteins and lipids in membranes, Biochim. Biophys. Acta 1376 (1998) 401–415.
[60] B.A. Lewis, D.M. Engelman, Lipid bilayer thickness varies linearly with acyl chain-length in fluid phosphatidylcholine vesicles, J. Mol. Biol. 166 (1983) 211–217.
[61] A. Zachowski, Phospholipids in animal eukaryotic membranes: transverse asymmetry and movement, Biochem. J. 294 (1993) 1–14.
[62] D. Marsh, A. Watts, R.D. Pates, R. Uhl, P.F. Knowles, M. Esmann, ESR spin-label studies of lipid–protein interactions in membranes, Biophys. J. 37 (1982) 265–274.
[63] N.J.P. Ryba, D. Marsh, Protein rotational diffusion and lipid/protein interactions in recombinants of bovine rhodopsin with saturated diacylphosphatidylcholines of different chain lengths studied by conventional and saturation-transfer electron spin resonance, Biochemistry 31 (1992) 7511–7518.
[64] A. Watts, Magnetic Resonance Studies of Phopsholipid–Protein Interactions in Bilayers, in: G. Cevc (Ed.), Phospholipids Handbook, CRC Press, 1993.
[65] J.F. White, J. Grodnitzky, J.M. Louis, L.B. Trinh, J. Shiloach, J. Gutierrez, J.K. Northup, R. Grisshammer, Dimerization of the class A G protein-coupled neurotensin receptor NTS1 alters G protein interaction, Proc. Natl. Acad. Sci. U. S. A. 104 (2007) 12199–12204.
[66] J.H. Bolivar, J.M. East, D. Marsh, A.G. Lee, Effects of lipid structure on the state of aggregation of potassium channel KcsA, Biochemistry 51 (2012) 6010–6016.
[67] A. Kusumi, J.S. Hyde, Spin-label saturation-transfer electron spin resonance detection of transient association of rhodopsin in reconstituted membranes, Biochemistry 21 (1982) 5978–5983.
[68] A.V. Botelho, T. Huber, T.P. Sakmar, M.F. Brown, Curvature and hydrophobic forces drive oligomerization and modulate activity of rhodopsin in membranes, Biophys. J. 91 (2006) 4464–4477.
[69] O. Soubias, K. Gawrisch, Probing specific lipid–protein interaction by saturation transfer difference NMR spectroscopy, J. Am. Chem. Soc. 127 (2005) 13110–13111.
[70] K. Mitra, I. Ubarretxena-Belandia, T. Taguchi, G. Warren, D.M. Engelman, Modulation of the bilayer thickness of exocytic pathway membranes by membrane proteins rather than cholesterol, Proc. Natl. Acad. Sci. U. S. A. 101 (2004) 4083–4088.
[71] F. Sixl, A. Watts, Headgroup interactions in mixed phospholipid bilayers, Proc. Natl. Acad. Sci. U. S. A. 80 (1983) 1613–1615.
[72] O. Soubias, W.E. Teague Jr., K.G. Hines, D.C. Mitchell, K. Gawrisch, Contribution of membrane elastic energy to rhodopsin function, Biophys. J. 99 (2010) 817–824.
[73] J.F. White, N. Noinaj, Y. Shibata, J. Love, B. Kloss, F. Xu, J. Gvozdenovic-Jeremic, P. Shah, J. Shiloach, C.G. Tate, R. Grisshammer, Structure of the agonist-bound neurotensin receptor, Nature 490 (2012) 508–513.
[74] T.W. Schwartz, T.M. Frimurer, B. Holst, M.M. Rosenkilde, C.E. Elling, Molecular mechanism of 7TM receptor activation—a global toggle switch model, Annu. Rev. Pharmacol. Toxicol. 46 (2006) 481–519.
[75] R. Nygaard, Y. Zou, Ron O. Dror, Thomas J. Mildorf, Daniel H. Arlow, A. Manglik, Albert C. Pan, Corey W. Liu, Juan J. Fung, Michael P. Bokoch, Foon S. Thian, Tong S. Kobilka, David E. Shaw, L. Mueller, R.S. Prosser, Brian K. Kobilka, The dynamic process of β_2-adrenergic receptor activation, Cell 152 (2013) 532–542.
[76] A. Manglik, Tae H. Kim, M. Masureel, C. Altenbach, Z. Yang, D. Hilger, Michael T. Lerch, Tong S. Kobilka, Foon S. Thian, Wayne L. Hubbell, R.S. Prosser, Brian K. Kobilka, Structural insights into the dynamic process of β_2-adrenergic receptor signaling, Cell 161 (2015) 1101–1111.
[77] C. Neale, Henry D. Herce, R. Pomès, Angel E. García, Can specific protein–lipid interactions stabilize an active state of the beta 2 adrenergic receptor? Biophys. J. 109 (2015) 1652–1662.
[78] A.M. Powl, J.M. East, A.G. Lee, Heterogeneity in the binding of lipid molecules to the surface of a membrane protein: hot spots for anionic lipids on the mechanosensitive channel of large conductance MscL and effects on conformation, Biochemistry 44 (2005) 5873–5883.
[79] A.M. Powl, J.M. East, A.G. Lee, Anionic phospholipids affect the rate and extent of flux through the mechanosensitive channel of large conductance MscL, Biochemistry 47 (2008) 4317–4328.
[80] A.M. Powl, J.M. East, A.G. Lee, Importance of direct interactions with lipids for the function of the mechanosensitive channel MscL, Biochemistry 47 (2008) 12175–12184.
[81] P. Marius, M. Zagnoni, M.E. Sandison, J.M. East, H. Morgan, A.G. Lee, Binding of anionic lipids to at least three nonannular sites on the potassium channel KcsA is required for channel opening, Biophys. J. 94 (2008) 1689–1698.
[82] J. Carney, J.M. East, S. Mall, P. Marius, A.M. Powl, J.N. Wright, A.G. Lee, Fluorescence Quenching Methods to Study Lipid–Protein Interactions, Current Protocols in Protein Science, John Wiley & Sons, Inc., 2001
[83] R.J. Froud, J.M. East, E.K. Rooney, A.G. Lee, Binding of long-chain alkyl derivatives to lipid bilayers and to $(Ca^{2+}$–$Mg^{2+})$-ATPase, Biochemistry 25 (1986) 7535–7544.
[84] H. Meves, Arachidonic acid and ion channels: an update, Br. J. Pharmacol. 155 (2008) 4–16.
[85] L. Boland, M. Drzewiecki, Polyunsaturated fatty acid modulation of voltage-gated ion channels, Cell Biochem. Biophys. 52 (2008) 59–84.
[86] K.L. Hamilton, C.A. Syme, D.C. Devor, Molecular localization of the inhibitory arachidonic acid binding site to the pore of hIK1, J. Biol. Chem. 278 (2003) 16690–16697.
[87] N. Decher, A.K. Streit, M. Rapedius, M.F. Netter, S. Marzian, P. Ehling, G. Schlichthorl, T. Craan, V. Renigunta, A. Kohler, R.C. Dodel, R.A. Navarro-Polanco, R. Preisig-Muller, G. Klebe, T. Budde, T. Baukrowitz, J. Daut, RNA editing modulates the binding of drugs and highly unsaturated fatty acids to the open pore of Kv potassium channels, EMBO J. 29 (2010) 2101–2113.
[88] J.H. Bolivar, N. Smithers, J.M. East, D. Marsh, A.G. Lee, Multiple binding sites for fatty acids on the potassium channel KcsA, Biochemistry 51 (2012) 2889–2898.
[89] N. Smithers, J.H. Bolivar, A.G. Lee, J.M. East, Characterizing the fatty acid binding site in the cavity of potassium channel KcsA, Biochemistry 51 (2012) 7996–8002.
[90] P. Gailly, M. Najimi, E. Hermans, Evidence for the dual coupling of the rat neurotensin receptor with pertussis toxin-sensitive and insensitive G-proteins, FEBS Lett. 483 (2000) 109–113.
[91] W. Liu, E. Chun, A.A. Thompson, P. Chubukov, F. Xu, V. Katritch, G.W. Han, C.B. Roth, L.H. Heitman, A.P. IJzerman, V. Cherezov, R.C. Stevens, Structural basis for allosteric regulation of GPCRs by sodium ions, Science 337 (2012) 232–236.
[92] A.D. Albert, K. Boesze-Battaglia, Z. Paw, A. Watts, R.M. Epand, Effect of cholesterol on rhodopsin stability in disk membranes, Biochim. Biophys. Acta 1297 (1996) 77–82.
[93] D.C. Mitchell, M. Straume, J.L. Miller, B.J. Litman, Modulation of metarhodopsin formation by cholesterol-induced ordering of bilayer lipids, Biochemistry 29 (1990) 9143–9149.
[94] K. Boesze-Battaglia, A.D. Albert, Cholesterol modulation of photoreceptor function in bovine retinal rod outer segments, J. Biol. Chem. 265 (1990) 20727–20730.
[95] M. Jafurulla, B.D. Rao, S. Sreedevi, J.-M. Ruysschaert, D.F. Covey, A. Chattopadhyay, Stereospecific requirement of cholesterol in the function of the serotonin$_{1A}$ receptor, Biochim. Biophys. Acta 1838 (2014) 158–163.
[96] M.A. Hanson, V. Cherezov, M.T. Griffith, C.B. Roth, V.P. Jaakola, E.Y.T. Chien, J. Velasquez, P. Kuhn, R.C. Stevens, A specific cholesterol binding site is established by the 2.8 A structure of the human b_2-adrenergic receptor, Structure 16 (2008) 897–905.
[97] H. Li, V. Papadopoulos, Peripheral-type benzodiazepine receptor function in cholesterol transport. Identification of a putative cholesterol recognition/interaction amino acid sequence and consensus pattern, Endocrinology 139 (1998) 4991–4997.
[98] M. Jafurulla, S. Tiwari, A. Chattopadhyay, Identification of cholesterol recognition amino acid consensus (CRAC) motif in G-protein coupled receptors, Biochem. Biophys. Res. Commun. 404 (2011) 569–573.
[99] A.G. Lee, Biological membranes: the importance of molecular detail, Trends Biochem. Sci. 36 (2011) 493–500.
[100] A. Manglik, B. Kobilka, The role of protein dynamics in GPCR function: insights from the β_2AR and rhodopsin, Curr. Opin. Cell Biol. 27 (2014) 136–143.

Please cite this article as: J.H. Bolivar, et al., Interaction of lipids with the neurotensin receptor 1, Biochim. Biophys. Acta (2016), http://dx.doi.org/10.1016/j.bbamem.2016.02.032